

# A COMPREHENSIVE REVIEW OF PEROVSKITE-BASED OPTO- ELECTRONIC DEVICES

IYASELE, Edgar Omondiale<sup>1</sup>

<sup>1</sup>*Department of Mechanical Engineering, Michael Okpara University of Agriculture, Umudike, Nigeria*

\*Corresponding Author: e-mail: [edgaromons2003@yahoo.com](mailto:edgaromons2003@yahoo.com) Tel +234-8135359855

## ABSTRACT

Perovskite based devices have gained significant attention recently owing to their excellent properties, low processing cost, and outstanding optoelectronic merits. Organic-inorganic metal halide Perovskites have been demonstrated to be promising materials in a variety of opto-electronic applications such as in light emitting devices (LEDs), lasers and photodetectors. This is attributed to the materials ability to benefit from the tunable bandgap resulting to high performance photon sources for lighting, display and communication technologies. In this comprehensive review, we looked at the organic-inorganic metal halide Perovskites Solar Cells in terms of its meaning, crystal structure, types and synthetic methods (films and phase formation, film quality). We also reviewed the recent advances of organic-inorganic metal halide Perovskite materials in opto-electronic devices. Applications including photo-detection, energy harvesting and light-emitting devices are then highlighted. We concluded by highlighting some ways to improve the stability of organic-inorganic metal halide Perovskite based opto-electronic devices and produce LEDs, lasers and photo-detectors systems that are of low-cost and high performance.

**Keywords:** Perovskites, Solar Cells, Devices, Organic-inorganic metal halide, Opto-electronic.

## 1. INTRODUCTION

Though a detailed overview of the historical evolution of PSC performance, occurring over a short time period, can be found in several review articles (Snaith 2013; Leijtens *et al.*, 2015; Yu and Sun, 2015, and Rong *et al.*, 2015), Perovskites have been known over a century ago (Green *et al.*, 2014), they received attention only when Miyasaka *et al.* used methylammonium lead halide (Perovskite) as a light harvesting material in excitonic solar cells (Kojima *et al.*, 2009). This group utilized Perovskite as sensitizers in dye sensitized solar cells (DSSC) and achieved the solar-to-power conversion efficiency of 3.2% for  $(\text{CH}_3\text{NH}_3)\text{PbBr}_3$  and 3.8%  $(\text{CH}_3\text{NH}_3)\text{PbI}_3$  (Kojima *et al.*, 2009). However, instability of these devices due to the degradation of Perovskites in liquid electrolyte containing lithium halide prompted Park *et al.* in 2011 to develop the quantum-dot sensitized solar cells using Perovskite  $(\text{CH}_3\text{NH}_3)\text{PbI}_3$  sensitizers (Im *et al.*, 2011). But these devices reduced the

performance of solar cell in a short span of time due to the dissolution of halides in liquid electrolyte (Im *et al.*, 2011). In order to avoid corrosive liquid electrolyte in Perovskite DSSC, Kim *et al.*, developed the solid-state electrolyte, spiro-OMeTAD (2,2',7,7'-tetrakis (N,N-di-p-methoxyphenylamine)- 9,9'-spirobifluorene), which can act as a hole transporting material (HTM) (Kim *et al.*, 2012).

The architecture of Perovskite solar cells was derived from the dye sensitized solar cell (DSSC) technology (Wang *et al.*, 2016). The traditional architecture of DSSCs consisted of a porous TiO<sub>2</sub> scaffold, sensitized by a dye and infiltrated by a liquid electrolyte. As regards the dye, Kojima *et al.* (2009) investigated CH<sub>3</sub>NH<sub>3</sub>PbBr<sub>3</sub> and CH<sub>3</sub>NH<sub>3</sub>PbI<sub>3</sub> as an alternative to replace it. This however yielded moderate success (Kojima *et al.*, 2009; Kojima *et al.*, 2006). Based on the inherent instability of these devices, Lee *et al.* in 2012 attempted to replace the TiO<sub>2</sub> scaffold, used to transport electrons, with an insulator (Al<sub>2</sub>O<sub>3</sub>) (Lee *et al.*, 2012). This demonstrated for the very first time that Perovskite material could effectively transport electrons without the underlying TiO<sub>2</sub> layer. With this insight, the demonstration of a planar geometry solar cell with a Perovskite thin film as the absorber layer evolved (Liu *et al.*, 2013). A high efficiency with this device structure was however achieved. The excellent optoelectronic properties of Perovskite make them attractive candidates to realize optoelectronic devices beyond solar cells, such as LEDs, lasers, and photodetectors. In this review, we discuss the synthetic methods of metal halide Perovskites and the recent advances of three types of optoelectronic devices, including LEDs, lasers and photodetectors.

The rapid advance of Perovskite solar cells has prompted the development of other types of Perovskite-based optoelectronics, including LEDs, lasers and photo-detectors (Green *et al.*, 2014; Yuan *et al.*, 2016; Xing *et al.*, 2014 and Fang *et al.*, 2015). Perovskite-based optoelectronic devices have gained significant attention due to their remarkable performance and low processing cost, particularly for solar cells. However, for Perovskite light-emitting diodes (LEDs), non-radiative charge carrier recombination has limited electroluminescence (EL) efficiency. Similar to conventional semiconductors, the luminescence efficiency of photo- or electrically-excited charge carriers in the Perovskite material is governed by the relative strengths of radiative and non-radiative processes (Baodan *et al.*, 2018). Since the first report of halide Perovskite LEDs in 2014, the device EQEs (external quantum efficiencies) have risen from ~0.1% to ~14% (Tan *et al.*, 2014; Yang *et al.*, 2018). While these high electroluminescence (EL) efficiencies are surprising for the solution-processed hybrid semiconductor containing a considerable level of grain-boundary and interfacial defects, such device performance still falls behind that of the best light-emitting diodes (OLEDs) which exhibit EQEs of more than 20% without enhanced optical outcoupling (Di *et al.*, 2017). Despite the good tolerance of the hybrid Perovskite materials family to electronic defects the EL efficiencies achieved to date suggest that the suppression of non-radiative recombination under electrical excitation conditions still remains a challenge (Ball and Petrozza, 2016). Non-radiative recombination is also an important mechanism for voltage loss in photovoltaic solar cells. An ideal open-circuit voltage predicted by the Shockley-Queisser model is only achievable with near-unity luminescence yield (Yablonovitch, 2016). To enhance radiative emission processes in LEDs, one of the most successful approaches is the use of low-dimensional structures such as nanocrystals and quasi-2D/3D nanostructures that are considered to confine charge carriers (Yuan *et al.*, 2016; Xiao *et al.*, 2017).

## 2. PHENOMENA

## 2.1 WHAT ARE PEROVSKITES?

Perovskite is a type of mineral that is chemically found on the earth crust. It was first discovered in the Ural Mountains and was named after a Russian noble man and mineralogist, Lev Perovski (founder of the Russian Geographical Society) (Dawn, 2016). The Perovskite solar cells have the same structure of the Perovskite mineral, hence named Perovskite solar cells. A Perovskite structure is anything that has the generic form  $ABX_3$  and the crystallographic structure as Perovskite (the mineral).

Depending on the atoms or molecules used in the structure, Perovskites may obtain a set of interesting properties like superconductivity, spintronics and catalytic properties. Hence, scientists and researchers finds Perovskites as exciting playground for physicists, chemists and material scientists.

## 2.2 CRYSTAL STRUCTURE

Perovskite are a family of materials with the crystal structure of calcium titanate, that is,  $ABX_3$  (Muhammad *et al.*, 2015). There are numerous materials which adopt this structure with exciting applications based on their thermoelectric, insulating, semi conducting, piezoelectric, conducting, antiferromagnetic and superconducting properties (Service, 2014).  $ABX_3$  describes the crystal structure of Perovskite class of materials, where A and B are cations and X is an anion of different dimensions with A being larger than X. Crystal structure of Perovskites is illustrated in figure 2.1 below:

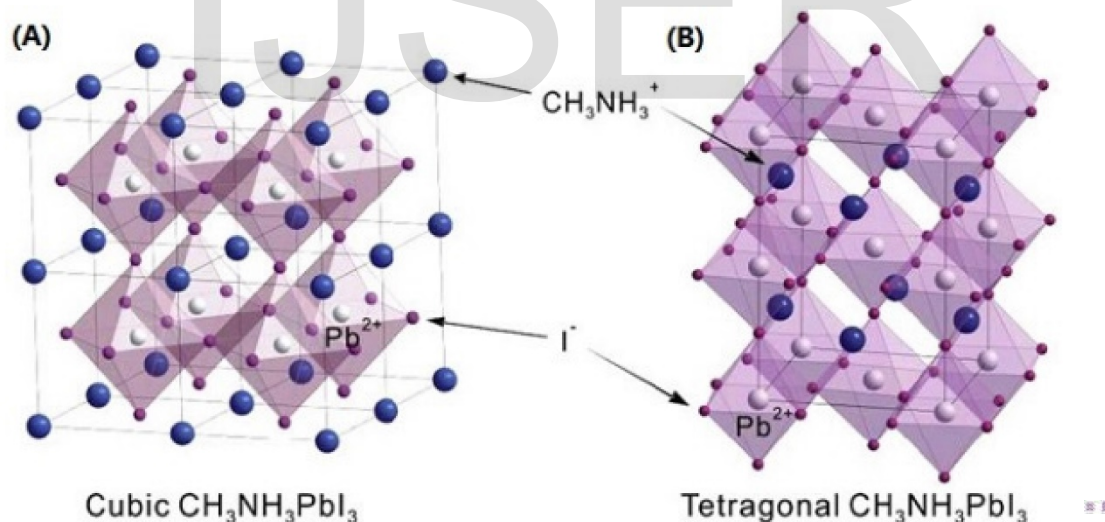


**Figure 1:** Crystal structure of Perovskite

**Source:** Shiqiang and Walid (2016).

The crystal structure of Perovskite can be alternatively viewed as corner-linked  $BX_6$  octahedral with interstitial A cation. Its crystallographic stability and apparent structure can be deduced by considering a Goldschmidt tolerance factor  $t$  and an octahedral factor  $N$ . The tolerance factor  $t$  is defined as the ratio of the distance  $A-X$  to the distance  $B-X$  in an idealized solid sphere model as shown in equation (1) below:

$$t = (R_A + R_X) / [\sqrt{2}(R_B + R_X)] \quad (1)$$

Where  $R_A$ ,  $R_B$  and  $R_X$  are the ionic radii of the corresponding ions.

The octahedral factor  $\mu$  is defined as the ratio  $R_B / R_X$ . For halide Perovskites ( $X = F, Cl, Br$  and  $I$ ),  $0.81 < \mu < 1.11$  and  $0.44 < \mu < 0.90$  are the typical values. Narrower range of  $t$  values from 0.89 to 1.0 dictates cubic structure, while lower values of  $t$  stabilizes as a less symmetric tetragonal and orthorhombic structure.

In case of  $ABX_3$ , the larger cation A is considered as an organic cation typically methylammonium ( $CH_3NH_3^+$ ) with  $R_A = 0.18\text{nm}$  (Li *et al.*, 2008), though ethylammonium ( $CH_3CH_2NH_3^+$ ,  $R_A = 0.23\text{nm}$ ) and formamidinium ( $NH_2CH = NH_2^+$ ,  $R_A = 0.19\text{-}0.22\text{nm}$ ) also provide excellent results. Anion X is a halogen such as iodine with  $R_X = 0.220\text{nm}$ , Bromine (Br) and chlorine (Cl) used in Perovskites with  $R_X = 0.196\text{nm}$  and  $0.181\text{nm}$  respectively though in a mixed halide configuration. For cation B, Lead (Pb) with  $R_B = 0.119\text{nm}$  and Tin (Sn) with  $R_B = 0.110\text{nm}$  have been used for high efficiency in PSCs because of lower theoretical ideal band gaps (Pang *et al.*, 2014). Although Sn has similar band gap with Pb and in the same group, due to the ease of oxidation and lack of stability, it performs poorly compared to Pb in efficiency.

## 2.3 TYPES OF PEROVSKITE SENSITIZED SOLAR CELLS

### 2.3.1 Perovskite Sensitized Solar Cells

DSSCs are the forerunners of Perovskite solar cells. In search of a more efficient light sensitizers for DSSCs, Miyasaka *et al.* reported the first Perovskite sensitized solar cells between 2006 and 2008.  $CH_3NH_3PbI_3$  and  $CH_3NH_3PbBr_3$  absorbers were employed with an iodide triiodide redox couple or a polypyrrole carbon black composite solid-state hole conductor. Full sun Power Conversion Efficiency (PCE) varying between 0.4 and 2% was measured for solid-state and liquid electrolyte cells, respectively (Kojima *et al.*, 2006).

In 2009, the first peer-reviewed report on Perovskite-sensitized solar cell was published with PCE of 3.5% (Kim *et al.*, 2012). In 2008, Kojima *et al.* decided to retain the liquid electrolyte reported earlier by Kim *et al.* the result was an improved efficiency of 6.5% (Kojima *et al.*, 2008). Owing to the instability and degradation within minutes of these cells, due to the liquid electrolyte, the idea of adopting a solid-state hole transport medium was born. Kojima *et al.* in 2006 attempted this but success was only made when Murakami, Miyasaka and Park in collaboration with Gratzel *et al.* developed the first solid-state Perovskite solar cells employing Spirobifluorene (spiro-OMeTAD) as the hole transporter (Kojima *et al.*, 2006). This cell recorded maximum full sun PCE of between 8 and 10% employing mixed halide Perovskites of iodine and chlorine (Kojima *et al.*, 2009).

### 2.3.2 Mesoporous $TiO_2$ structures

The first use of hybrid Perovskite absorbers in photovoltaic cells is based on the typical structure of a dye-sensitized solar cell, where the Perovskite absorber is self-assembled within the gaps of a porous  $TiO_2$  layer formed by sintering nanoparticles (Song *et al.*, 2015). The typical configuration of this type of Perovskite based solar cells FTO / Mesoporous  $TiO_2$  / Perovskite / (spiro-OMeTAD) / electrode is as shown below in figure 2

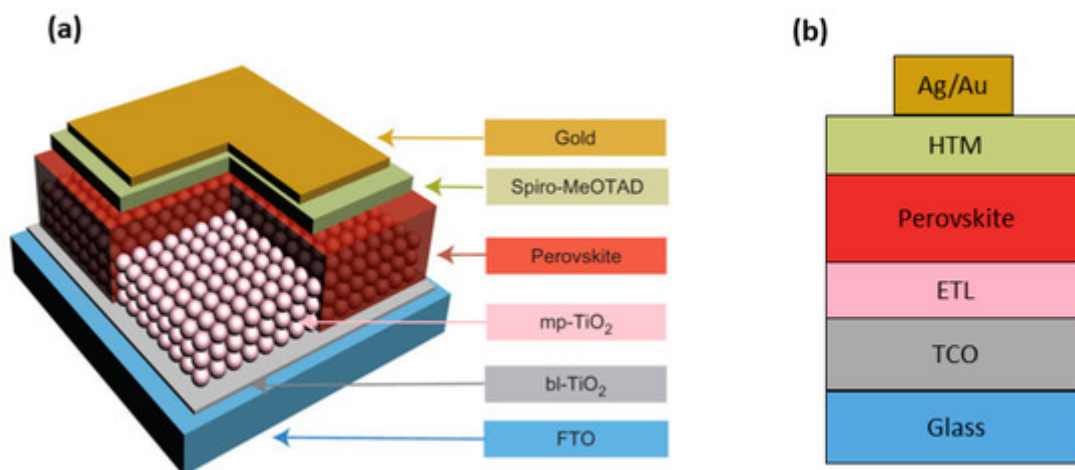


**Figure 2:** Schematic Diagram and Cross Section of the Mesoporous Structured PSC Device

**Source:** Paola *et al.* (2017).

In this structure, Perovskite materials are deposited onto Mesoporous TiO<sub>2</sub>, which is used to facilitate electron transport between the Perovskite absorber and the FTO (fluorine-doped Tin oxide) electrode. A subsequent work demonstrated the replacement of the relatively conductive porous TiO<sub>2</sub> with an insulating porous Al<sub>2</sub>O<sub>3</sub> layer (Song *et al.*, 2015). It is however important to note that successful pore-filling in these structures is necessary in order to prevent leakage via the device, which has been an issue for thick Mesoporous structures.

The use of Mesoporous structures as a scaffold to fabricate Perovskite solar cells has led to an increase in device performance from 3.8% to over 17% PCE within a few years (Kojima *et al.*, 2009). Just as this structures do not rely on long carrier diffusion length; it is also able to provide a compensation platform for the investigation of new Perovskite materials (Song *et al.*, 2015). While the use of a Mesoporous scaffold requires a comparatively complex device architecture and fabrication process in which many problems could arise, it has consistently delivered high efficiencies that made its use fully worthwhile for laboratory scale investigations (Song *et al.*, 2015).

### 2.3.3 Planar Structure

In a planar junction Perovskite solar cell, a several hundred nanometer thick absorber layer, is sandwiched between the electron transport layer (ETL) and hole transport layer (HTL) without a Mesoporous scaffold (Song *et al.*, 2015). These cells can deliver efficiency values of over 15% despite being under developed for an even shorter period than their Mesoporous counterparts. This architecture offers the advantages of a simplified device configuration and fabrication procedure, and thus, rapidly acquired the interest of the thin film research community. Planar structures are most commonly illuminated from the n-type side, resulting in the structure glass/TCO/ETL/Perovskite/HTL/metal or p-type side, resulting in the inverted structure glass/TCO/HTL/Perovskite/ETL/metal which functions in a superstrate configuration. Owing to its simplified fabrication and ease of deposition, the planar architecture provides a great promise in future applications, including high performance flexible and portable devices (Song *et al.*, 2015).

### 2.3.4 Mesosuperstructured PSCs (MSSC)

These are PSC device structures having  $\text{CH}_3\text{NH}_3\text{PbI}_2\text{Cl}$  mixed Perovskite, coated with alumina layer in a photovoltaic cell. Bi *et al.*, reported that the PCE of this type of structure reached 10.9% in 2013 (Bi *et al.*, 2013). They were so called because the photogenerated electrons are not transferred to alumina because of the difference in band edges of alumina and Perovskite active layer, which acts only as a scaffold for carrying the photoactive layer (Muhammed *et al.*, 2015). The scaffold layers afford processing at lower temperatures by excluding high temperatures annealing step as neither generated electrons are injected into the Mesoporous layer nor transported. With the advantage of processing at lower temperatures, Lee *et al.* reported a MSSC/PCE value of 12.3% (Though  $\text{Al}_2\text{O}_3$  Mesoporous layers was dried at  $150^\circ\text{C}$ ) (Lee *et al.*, 2012).

### 2.3.5 Hybrid Perovskite Solar Cells

An example of a hybrid planar heterojunction solar cell is a device structure based on  $\text{TiO}_2\text{CH}_3\text{NH}_3\text{PbI}_{3-x}$  / P3HT (poly (3-hexylthiophene)). Such device achieved a better photovoltaic performance when the ITO (indium-doped-Tin-oxide) substrate was treated with C60 self-assembled monolayer having an improved PCE of 6.7%. This was achieved with a significant increase in both  $J_{sc}$  (shunt current density) and  $V_{oc}$  (open circuit voltages) (Jeng *et al.*, 2013). The active layer of a hybrid planar heterojunction cell can be sandwich between poly (N,N<sup>1</sup>-bis (4-butylphenyl) – N, N<sup>1</sup>-bis (phenyl)- benzidine)(poly-TPD) as Hole transporting material layer and electron accepting PCBM layer (Abrusci *et al.*, 2013). A PCE of 12% was thus reported.

### 2.3.6 Flexible Perovskite Solar Cells

If the commercialization goal of PSCs must be achieved, further studies on the possibilities of fabricating cells and flexible substrate must be encouraged. However, several works have been done in this field owing to the low temperature solution processability of PSCs. Ability to conform to the contours of the platform holds obvious promises for incorporation of this technology in diverse application (Muhammad *et al.*, 2015). Docampo *et al.*, in 2013 achieved a higher PCE of 10.2% using device structure ITO / ZnO (25nm) /  $\text{CH}_3\text{NH}_3\text{PbI}_3$  / Spiro- MeoTAD / Ag, fabricated using low temperature solution processing techniques (Docampo *et al.*, 2013).

### 2.3.7 Hybrid Multijunction Solar Cells

Song *et al.*, concluded in the work saying it is anticipated that the demonstration of new solar technologies based on Perovskites, or the integration of an established manufacturing method that uses both Perovskite and existing technologies are particularly promising for the future photovoltaic market (Song *et al.*, 2015). They envisaged a tandem cell configuration where PSCs can be used effectively as a top cell with existing technologies and at very little optimization in terms of bandgap widening and Fill Factor (FF) enhancement (Mailoa *et al.*, 2015). With a reasonable estimate of achieving  $20\text{mAc m}^{-2}$  and  $V_{oc}$  of 1.1V at the top Perovskite cell, a silicon cell generating 0.75V  $V_{oc}$  will lead to a FF of 0.8 and efficiency of 29.6% (Snaith, 2013). Tandem solar cells have attracted the attention of researchers around the world as it offers an alternative path towards higher efficiencies when compared to those obtained from single solar cell structures. For a good tandem solar cell structure, an optimized top and bottom cell structure must be used in order to achieve maximum conversion efficiency (Olopade *et al.*, 2015).



### 3. SYNTHETIC METHODS

Perovskite solar cells can be manufactured with simpler wet chemistry techniques in a traditional laboratory environment, unlike silicon solar cells that need expensive, multi-step processes requiring an extreme temperature and vacuum controlled system. Perovskites can be created using a variety of solvent techniques and vapour deposition methods (Dawn, 2016). Approaches reported for the synthesis of Perovskite active layers are: one-step precursor solution deposition; two-step sequential deposition; dual-source vapour deposition; vapour assisted solution process; and sequential vapour deposition (Liu *et al.*, 2013; Burschka *et al.*, 2013; Hu *et al.*, 2014). Categorically, we can put the synthesis methods of Perovskite under these broad heading: solvent techniques (solution processing); vapour assisted solution processing and vacuum deposition.

#### 3.1 PEROVSKITE FILM FORMATION

Various processing techniques have been documented to fabricate hybrid Perovskite films. The major methods of fabricating Perovskite solar cells as suggested by Ezike *et al.* (2017) are Spin – coating, Vapour deposition and thermal evaporation methods. Spin-coating methods include one – step, two – step/ sequential deposition and vapour deposition method which include vapour - assisted deposition ,and dual – source vapour deposition, and thermal evaporation technique (dual source approach) have been used to prepare  $\text{CH}_3\text{NH}_3\text{PbX}_3$  materials (Ezike *et al.*, 2017).

It has also been suggested that the optoelectronic properties of Perovskite films are closely related to the processing conditions, such as the starting material ratio and the atmospheric conditions during film growth, which lead to a substantial difference in the film quality and device performance (Wang *et al.*, 2014). Hybrid Perovskite materials form with crystallinity, even when processed at low temperatures, and the formation of the final Perovskite phase benefits from the relatively high reaction rates between the organic and inorganic species. These advantages substantially expand the choices of available processing methods such as thermal evaporation and solution processing, and facilitate the adoption of new and varied architecture (Song *et al.*, 2015).

In solution processing of Perovskite film, a mixture of  $\text{MX}_2$  (M=Pb, Sn; X=Cl, Br, I) and AX (A= methyl-ammonium, MA; Formamidinium, FA) is dissolved in an organic solvent and deposited directly to form a film and followed by thermal annealing to produce the final Perovskite phase (You *et al.*, 2014).

In thermal evaporation synthesis of Perovskite film, a dual source is employed for  $\text{MX}_2$  and AX with different heat temperatures to form the Perovskite film (Liu *et al.*, 2013). Both solution processing and thermal evaporation methods described above are one-step processing methods. In one -step method, both the organic and inorganic halides are stoichiometrically prepared in a common solution and are then spin coated into a thin film. In sequential deposition synthesis of Perovskite films,  $\text{MX}_2$  layer such as  $\text{PbI}_2$  and an AX such as Methylammonium iodide (MAI) are deposited sequentially followed by heat treatment to form the completed Perovskite film (Xiao *et al.*, 2014). The deposition of the  $\text{MX}_2$  is done by spin-coating while AX can be introduced by spin-coating the AX solution on top of the  $\text{MX}_2$  layer or the AX solution can be immersed in  $\text{MX}_2$  layer to induce a solid-liquid reaction or by exposing the  $\text{MX}_2$  layer to AX vapour at elevated temperatures

(Pang *et al.*, 2014). Spin-coating deposition processes allow metal halide and organic halide to be dissolved in organic solvents which is followed by deposition on a substrate from which the formation of the Perovskite is achieved through annealing around 100°C. This method is a low-cost approach but it wastes a lot of precursors.

Two-step sequentially deposition can be carried out in thermal evaporation, by sequential deposition the inorganic and organic components. Here, the  $\text{PbI}_2$  is first spin-casted followed by solution processing or vacuum assisted deposition of MAI (Hu *et al.*, 2014). It is a heterophase reaction resulting in conversion to  $\text{MAPbI}_3$ . A modification of two-step deposition method is the vapour assisted growth of MAI on the  $\text{PbI}_2$  film. Compact and uniform  $\text{PbI}_2$  film obtained by solution processing is exposed to MAI vapour under ambient conditions. In contrast to vapour depositing, this method does not require expensive vacuum equipment and environmental controls. Combining the advantages of solution processing and low temperature vapour deposition, the films grown are pinhole-free offering higher efficiencies (Hu *et al.*, 2014; Xiao *et al.*, 2014). In vapour deposition method, the substrate is exposed to one or more volatile precursors, which react with the substrate and/or decompose to produce the wanted deposit. It can be when the metal halide is deposited by spin-coating or other methods and volatile organic halide is deposited by ejecting it to give out vapour in the reaction chamber (Ezike *et al.*, 2017). The vapour process is argued to be better than the solution process in planar heterojunction layout because the former produces a flat and even surface (Kestinro *et al.*, 2017).

Dual source vapour deposition method involves simultaneous evaporation of organic and inorganic salts from respective sources at high vacuum. PCE of ~12% was achieved using this method (Liu *et al.*, 2013). Dual source of organic and inorganic halide ejects the vapours to the substrate exposed in the chamber. It is a low-cost method, uniform step coverage, fast deposition, low processing temperature and high throughput.

Thermal evaporation is widely used as a technique for the preparation of thin films for deposition of metals, alloys and many compounds. The requirement is to create vacuum environment where enough heat is given to the evaporants to attain the vapour pressure required for evaporation (Abbas *et al.*, 2015).

### 3.1.1 Synthesis of Perovskite-Sensitized Solar Cells

A typical DSSC is a Mesoporous n-type Titania sensitized with a light absorbing dye in a redox active electrolyte. It was in the process of finding a more efficient light sensitizers for DSSCs that Miyasaka *et al.* reported the first Perovskite-sensitized solar cells, which they formed employing  $\text{CH}_3\text{NH}_3\text{PbI}_3$  and  $\text{CH}_3\text{NH}_3\text{PbBr}_3$  absorbers with an iodide triiodide redox couple (Kojima *et al.*, 2006).

### 3.1.2 Synthesis of Mesoporous $\text{TiO}_2$ Structures

A typical fabrication procedure for Mesoporous scaffold-based Perovskite solar cells involves the use of FTO substrates with a compact  $\text{TiO}_2$  blocking layer and a Mesoporous oxide layer that have each undergone high temperature sintering steps (500°C). In solution processing, Dawn, 2016 gave an elaborate explanation of the procedures as follows: the FTO substrates are cleaned in an ultrasonic bath with a combination of methanol and acetone and finally dried with Nitrogen gas. After the preparation of FTO substrates, the 0.15M and 0.3M  $\text{TiO}_x$  precursor solutions are prepared from titanium diisopropoxide bis (acetyl acetone) (0.0055mL and 0.11mL) with 1-butanol (1 mL). The initial step is to spin-coat 0.15M  $\text{TiO}_x$  precursor solution on the FTO glass substrate



at 3000rpm for 30 seconds, and annealed at 125°C for 5 minutes. This 0.30M solution process is performed twice, after which the FTO substrate is sintered at 500°C for 30 minutes to form a compact TiO<sub>2</sub> layer.

To prepare the Mesoporous TiO<sub>2</sub> layer, a TiO<sub>2</sub> paste is made using TiO<sub>2</sub> powder (100mg) and polyethylene glycol (10mg) in ultrapure water (0.5mL). This solution is then mixed with acetyl acetone (10.0μL) and triton X-100 (5 μL) for 30 minutes and left for 12 hours. This helps in suppressing the formation of bubbles in the solution. The TiO<sub>2</sub> paste obtained is coated on the substrate by spin-coating at 5000rpm for 30 seconds. The cells are annealed at 120°C for 5 minutes and at 500°C for 30 minute. To syntheses methyl ammonium iodide (CH<sub>3</sub>NH<sub>3</sub>I), 23.2mL of methylamine (CH<sub>3</sub>NH<sub>2</sub>) is reacted with 25.0mL of hydroiodic acid at 0°C for 2 hours with stirring. The precipitate is collected by removing the solvents at 50°C for 1 hour. The product obtained is re-dissolved and stirred in diethyl ether for 30 minutes to remove any impurities and dried using a rotary evaporator at 60°C for 3 hours. The CH<sub>3</sub>NH<sub>3</sub>I thus produced is finally dried in a vacuum.

To prepare Methylammonium lead iodide (CH<sub>3</sub>NH<sub>3</sub>PbI<sub>3</sub>) with a Perovskite structure, a solution of CH<sub>3</sub>NH<sub>3</sub>I (98.8mg) and PbI<sub>2</sub> (289.3mg) at a mole ratio of 1:1 in *n*-butyroactone (0.5mL) is mixed at 60°C. The CH<sub>3</sub>NH<sub>3</sub>PbI<sub>3</sub> solution is then introduced into the TiO<sub>2</sub> Mesoporous using a spin-coating method and annealed at 100°C for 15 minutes. Next step is to prepare the Hole-transport layer (HTM) by spin-coating. A solution of spiro-OMeTAD (36.1mg) in chlorobenzene (0.5mL) is mixed with a solution of lithium bis (trifluoromethylsulfonyl) imide (260mg) in acetonitrile (0.5mL) for 12 hours. This solution and 4-tert-butylpyridine (4μL) is then mixed with the Li-TFSL solution (8.8 μL) for 30 minutes at 70°C. All procedures are carried out in air. Finally, gold (Au) metal contacts is evaporated onto the sample as top electrodes. Figure 3 below shows the above detailed process.

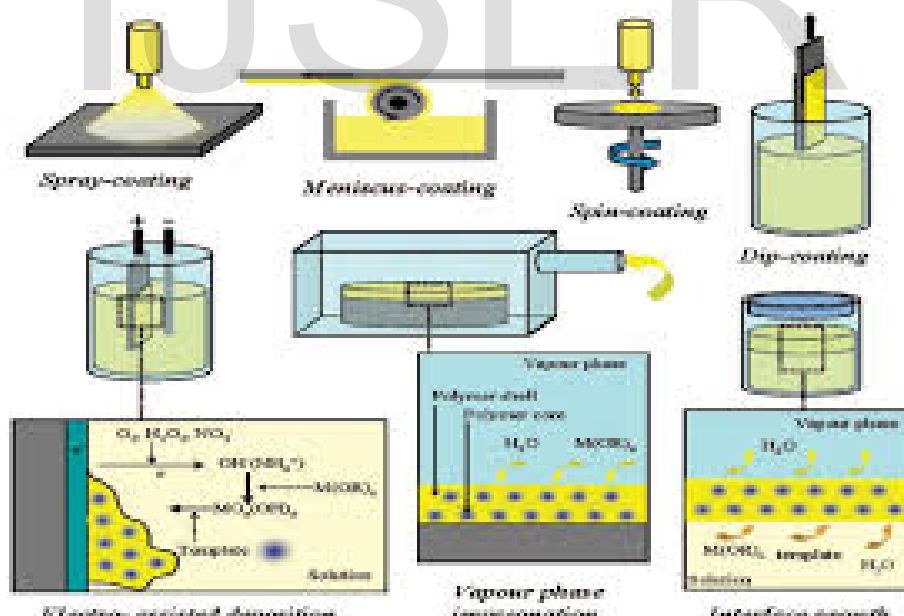


**Figure 3:** Synthesis of Mesoporous TiO<sub>2</sub> Structures

**Source:** Luther and Ranjit (2014).

### 3.1.3 Synthesis of Planar Structure

As earlier stated, planar junction PSCs have a several hundred nanometer thick absorber layer which is sandwiched between ETL and HTL without a Mesoporous scaffold. This architecture offers the advantages of a simplified device configuration and fabrication procedure. These structures are mostly commonly illuminated from the n-type side, resulting in the structure glass/TCO/ETL/Perovskite/ETL/metal (Jeng *et al.*, 2013; Chiang *et al.*, 2014).

The earliest attempts to fabricate planar Perovskite solar cells used single step deposition to deposit the Perovskite absorber layer. Compared to the Mesoporous scaffold, thermal evaporation can be more efficiently applied in a planar configuration, without worrying about the difficulty of Perovskite precursors penetrating into the Nanoporous scaffold. Bi *et al.*, 2013 attempted by thermal co-evaporation of  $\text{CH}_3\text{NH}_3\text{I}$  and  $\text{PbCl}_2$  and deposited  $\text{CH}_3\text{NH}_3\text{PbI}_{3-x}\text{Cl}_x$  onto FTO with a thin  $\text{TiO}_2$  layer resulting in a PCE of 15.4% (Bi *et al.*, 2013).

### 3.1.4 Synthesis of Meso Supers Structured PSCs (MSSC)

These devices are fabricated by spin-coating  $\text{CH}_3\text{NH}_3\text{PbI}_2\text{Cl}$  mixed Perovskite with alumina layer in a photovoltaic cell. A Mesosuperstructure concept was evaluated using  $\text{ZrO}_2$  Mesoporous scaffold with  $\text{CH}_3\text{NH}_3\text{PbI}_3$  light harvester which exhibited significant photovoltaic activity  $V_{oc}$  of approximately 900mV through lower than titania (Kim *et al.*, 2013).

### 3.1.5 Synthesis of Hybrid Perovskite Solar Cells

This is a device structure based on  $\text{TiO}_2/\text{CH}_3\text{NH}_3\text{PbI}_{3-x}\text{Cl}_x/\text{P3HT}$ , with the incorporation of self-assembled monolayer (e.g. C60). Here, the ITO substrate is treated with the C60 self-assembled monolayer (Jeng *et al.*, 2013). The concept of hybrid planar heterojunction cell incorporating 285nm thick layer of  $\text{CH}_3\text{NH}_3\text{PbI}_3$  was investigated by Abrusci *et al.*, 2013. Active layer was sandwiched between hole-transporting poly (N,N<sup>1</sup>- bis(4-butylphenyl)-N,N<sup>1</sup>-bis (phenyl)-benzidine) (poly-TPD) layer (10nm) and electron accepting PCBM layer (10nm). The charge collecting layers were solution-processed in spin-coated chlorobenzene while the active layer was vacuum-deposited by heating reagents  $\text{CH}_3\text{NH}_3\text{I}$  to 70°C and  $\text{PbI}_3$  to 250°C.

### 3.1.6 Synthesis of Flexible Perovskite Solar Cells

These PSCs consist of fabricating the cells on flexible substrates. Malinkiewicz *et al.*, 2014 investigated this using both regular and inverted device architecture on an ITO coated PET substrate. A  $\text{CH}_3\text{NH}_3\text{PbI}_{3-x}\text{Cl}_x$  active layer with PEDOT: PSS and PCBM as hole-transporting and electronic selective contacts were used. A PCE of 6.4% was achieved (Malinkiewicz *et al.*, 2014). A higher PCE of 10.2% was achieved using device structure of ITO/ZnO (25nm)/ $\text{CH}_3\text{NH}_3\text{PbI}_3$ / Spiro-OMeTAD/AG, fabricated using low temperature solution processing methods (Docampo *et al.*, 2013).

## 3.2 PEROVSKITE PHASE FORMATION

Depending on the relative sizes of the cation and the octahedron in a Perovskite structure, the Perovskite phase can be three dimensional (3D), two-dimensional (2D) or even one-dimensional (1D) in crystal structure (Stoumpos *et al.*, 2013).

Focusing on 3D organo-metal halide Perovskite phases, it is worth noting that the formation of

Perovskite structures usually follows the overall reaction formula  $AX + BX_2 \rightarrow ABX_3$ . Using this reaction as a typical example, it has been observed that the reaction kinetics of Perovskite phase formation are very fast (Liu and Kelly, 2013). During the transformation into the Perovskite lattice, spaces are formed between the layered  $PbI_6$  octahedral that share facets with  $PbI_2$  to create  $PbI_6$  octahedral that share only vertices in  $MAPbI_3$ . Solution of  $PbI_2$  is another important parameter that affects the intermediate reaction stage. Since it has been demonstrated that the soft Pb can easily coordinate with a variety of small molecules such as ethanolamine or dimethyl sulfoxide (DMSO), after which the original facet-sharing ( $PbI_6$ ) octahedral are partially disintegrated and small ligands are inserted, it is therefore logical to conclude that during the dissolution of  $PbI_2$ , solvent molecules partially replace iodine to ligate with lead, thus facilitating the subsequent reaction forming the Perovskite phase.

Besides the kinetics of phase formation, another issue is the formation of mixed-cation, mixed group IV metal, and mixed-halide Perovskite phases, allowing for the fine tuning of the optical and electronic properties of the final material (Song *et al.*, 2015). A Perovskite phase with mixed-group IV metals has recently been synthesized using MAI and a mixture of  $PbI_2$  and  $SnI_2$  (Hao *et al.*, 2014).

$MAPbX_3$ -based Perovskite have been found to exhibit multiple phases as a function of temperature and composition. These different phases possess dramatically different electrical/optical properties as well as stability. Stoumpos *et al.*, showed that  $MAPbI_3$  exhibited an X-phase,  $\delta$ -phase and  $\gamma$ -phase with transition temperature of  $400^0K$ ,  $333^0K$ , and  $180^0K$  respectively (Stoumpos *et al.*, 2013). Phase transformation can also occur in mixed halide systems. A mixed halide  $MAPbI_{3-x}Br_x$  ( $0 \leq X \leq 3$ ) was used for band-gap tuning and it was observed that the crystal structure transformed from the tetragonal phase to a cubic phase when the percentage of Br present passed a threshold of approximately X approximately 0.5 (Noh *et al.*, 2013). This phase transition has been presumed to explain the improved stability of  $MAPbI_{3-x}Br_x$  materials in the air and humidity test, making it an interesting addition to our understanding of the specifics of the Perovskite lattice.

### 3.3 PEROVSKITE FILM QUALITY

Based on various processing approaches, Perovskite materials exhibit a wide range of film properties like grain size, morphology, crystallinity, surface coverage, etc. Several works have also shown that Perovskite films exhibit composition/structure dependent properties (Song *et al.*, 2015). Therefore, since it is essential to achieve fine control over the reaction between the inorganic and organic species so as to produce Perovskites within the required properties, various process parameters have to be incorporated. Paramount among these are: stoichiometry, thermal treatment, solvent engineering, additives and environmental control.

The stoichiometry, particularly the ratio of the organic to inorganic component, largely affects the resulting  $MAPbI_{3-x}Cl_x$  film quality in terms of film conformity and carrier behaviour. Generally, a solution of  $PbX_2$  and MAX with a stoichiometry of 1:1 is used as the precursor to form a pure Perovskite phase (Song *et al.*, 2015). Further studies on film formation based on stoichiometry effects have also been conducted, in terms of the phase, the underlying reaction, and the possible byproducts. Details about this can be found in the works of Lee *et al.* (Lee *et al.*, 2012).

Thermal annealing is an essential step to initiate or accelerate the reaction between the molecules, as well

as the film formation. A delicate control of heat treatment is needed due to the fast reaction rate between the organic-inorganic component and their various phase in the low temperature of hybrid Perovskite range materials. Eperon *et al.*, investigated the properties of mixed halide Perovskite  $\text{MAPbI}_{3-x}\text{Cl}_x$  planar films based on one-step solution processing at different annealing temperatures (Eperon *et al.*, 2013). The authors observed that the higher the annealing temperature, the lower the film surface coverage. Liang *et al.* added 1% of 1, 8, diiodooctane (Dio) into a Perovskite precursor solution and demonstrated an increase in device performance in contrast to devices based on precursors without additives (Liang *et al.*, 2014). The films exhibited improved surface coverage and crystallinity as observed using SEM and XRD, respectively. This result showed that the inclusion of small amounts of chemical additives in Perovskite precursor solutions can provide advantages in terms of crystallinity, film coverage, and the resulting device performance. It also showed that the film growth can be effectively controlled.

Generally, Perovskite films are deposited and annealed in nitrogen or dry air glove boxes with  $\text{H}_2\text{O}$  levels

less than 5ppm, as the presence of moisture was deduced to deteriorate the Perovskite film. However, Zhou *et al.* found that Perovskite films annealed in a mild moisture environment of approximately 30% humidity. And could improve film properties significantly (Zhou *et al.*, 2014). The speculation is that the moisture could enhance film formation by partially dissolving the reaction species and accelerating mass transport within the film. It could also possibly promote the movement of organic species and accelerate the grain growth resulting in less pinholes in the films. This results indicate that a controlled atmosphere during the film formation will result in high performance Perovskite devices. The quality of hybrid Perovskite films can be determined by the critical role solvents play in all kind of solution processes. The selection of solvents with sufficient solubility for organic and inorganic precursor components is limited due to their distinct nature (Song *et al.*, 2015). Currently, DMF, DMSO, GBL and their mixtures are majorly used. These solvents have been shown to improve the film optoelectronic properties and device performance (Kim *et al.*, 2012; Zhan *et al.*; 2014). Kim *et al.*; reported that mixed solvents have improved the morphology of the Perovskite film (Kim *et al.*; 2014). Therefore, the solvents either from the precursor solution or induced during the processing, substantially influencing the molecule/species interaction within the system, and the subsequent film quality.

## 4. OPTO-ELECTRONIC DEVICES

### 4.1 LIGHT EMITTING DIODES

Baodan *et al.* (2018) explored the optoelectronic and photophysical properties of a Perovskite-polymer bulk heterostructure (PPBH). They prepared the emissive heterostructure from a combination of quasi-2D/3D Perovskites and a wide optical gap polymer. The absorption profile of the PPBH contained a distinct excitonic peak at ~575 nm, corresponding to the quasi-2D Perovskite with a formula of  $\text{A}_2\text{B}_{m-1}\text{PbmI}_{3m+1}$ , where A and B are organic cations. The absorption tail of the PPBH sample extended to ~800 nm, which they attributed to the quasi-3D phase. The photoluminescence (PL) spectrum of the sample peaked at ~795 nm (~1.56 eV), with a full-width-at-half-maximum (FWHM) of ~55 nm. Grazing-incidence wide-angle X-ray scattering (GIWAXS)

measurements indicated that the Perovskite crystallites are isotropically oriented in the PPBH film. High-resolution transmission electron microscopy (HR-TEM) results suggested the presence of quasi-2D/3D crystal structures (Weller *et al.*, 2015). From the X-ray diffraction (XRD) data, the average crystallite size was estimated to be 30-55 nm based on the FWHM of the diffraction peaks. The average surface roughness of the film is ~3.3 nm. To investigate the electroluminescence (EL) properties of the PPBH, they developed a solution-processed multilayer LED structure. The EL spectrum of the PPBH LED was nearly identical to that of the steady-state PL, exhibiting a slightly narrower FWHM of ~49 nm. The low onset of radiance ( $10^{-4}$  W sr<sup>-1</sup> m<sup>-2</sup> at 1.3 V) indicated that the LED structure allows barrier-free bi-polar charge injection into the emissive layer. The peak EQE of best devices reached 20.1%, representing a record for Perovskite-based LEDs (Wang *et al.*, 2015). The angle-dependent EL intensities exhibited a Lambertian profile, allowing accurate estimation of EQEs. As the drive voltages are low, the wall-plug efficiency (electricity-to-light power-conversion efficiency) is also high, reaching 16.2%. The efficiencies of their Perovskite-based LEDs were on par with those of the best OLEDs and quantum-dot (QD) LEDs (Di *et al.*, 2017). For devices encapsulated in epoxy adhesive/cover glass, the EL half-life in air under continuous operation at the current density corresponding to the peak EQE point (0.1 mA cm<sup>-2</sup>) has reached 46 hours. Although practical applications demand further improvements, the half-life of their devices represents the longest operational lifetime observed for Perovskite-based LEDs to date (Xiao *et al.*, 2017). Concluding they recommended that, while an EQE of over 20% for PPBH LEDs can be accounted for within the conventional outcoupling model, photon recycling provides prospects of further efficiency improvements.

The authors successfully demonstrated PPBH LEDs with high EQEs of up to 20.1% and an EL half-life of 46 hours (Baodan, 2018). They represent the most efficient Perovskite-based LEDs to date, and are comparable with some of the best OLEDs and QD LEDs (Di *et al.*, 2017). Transient optical experiments suggested that in the PPBH system, localized higher-energy excitations dissociate into charges at lower-energy sites within ~1 ps, significantly faster than the ~100 ps energy funneling time reported for quasi-2D/3D Perovskites (Yuan *et al.*, 2016). The ultrafast migration of excitations observed ensures that any non-radiative traps with energies above the final emissive species are rendered insignificant, as these loss processes need to compete kinetically with the rapid excitation transfer. After the rapid energy migration, emission occurred primarily through a bimolecular recombination channel. PPBH thin films with/without charge-transport contacts exhibit a PL decay tail (monomolecular) lifetime of ~1.5  $\mu$ s, comparable to or exceeding that observed for Perovskite single crystals indicating low trap densities in these structures (Brenner *et al.*, 2016). Bulk and interfacial non-radiative relaxation processes were effectively suppressed, leading to the excellent EQEs and near-100% PLQEs. Optical outcoupling from the emissive layer was improved by the reduced effective refractive index, and their measured EQE was consistent with this conventional model for thin-film LEDs. However, low absorption losses for modes guided in-plane may enable performance enhancement through photon recycling that allows outcoupling from these modes (Pazos-Outon *et al.*, 2016). The authors anticipate the outstanding optoelectronic properties of the PPBH system to lead to low-cost and high-performance photon sources for lighting, display and communication technologies.

## 4.2 LASERS

Sun *et al.* (2018) reported that Since the first invention of ruby-laser (Cr:Al<sub>2</sub>O<sub>3</sub>) by Maiman in 1960 and later

neodymium-doped yttrium aluminium garnet (Nd:YAG) lasers in 1970s, solid-state lasers have become a key technology for communication, materials fabrication, medical care, and optical imaging processing (Sun *et al.*, 2018). To date, a rich variety of materials have been applied in lasers with emission from the ultraviolet to near-infrared region such as ZnO, GaN, CdS, and GaAs (Bagnall *et al.*, 1997).

In recent years, organic–inorganic metal halide Perovskite materials have been proven to be a promising optical gain material for lasers (Sun *et al.*, 2018). Meanwhile organic–inorganic hybrid Perovskite can be fully deposited by simple solution-based methods and particularly, single crystal organic–inorganic hybrid Perovskite can be acquired by solution growth. Recently, several works have reported on the fabrication of room-temperature single crystal Perovskite lasers. (Cha *et al.*, 2016). A recent work suggested that Perovskite films can also possess excellent optical gain in a wide range of wavelengths (Chen, *et al.*, 2011).

Xing *et al.* studied the intrinsic gain of Perovskites by examining the amplified spontaneous emission (ASE) in a cavity-free configuration (Xing *et al.*, 2014). As a result of low bulk defect density in  $\text{CH}_3\text{NH}_3\text{PbI}_3$  films, the ASE threshold carrier density was calculated to be as low as  $\approx 1.7 \times 10^{18} \text{ cm}^{-3}$ , which means that this device can obtain adequate gain and results in an efficiency laser.

Random lasing in planar  $\text{MAPbI}_3$  Perovskite was achieved by Dhanker *et al.* (2014). They found low lasing thresholds  $< 200 \mu\text{J cm}^{-2}$  per pulse and narrow linewidth ( $\Delta \lambda < 0.5 \text{ nm}$ ). The low threshold coherent random lasing shows that the lead halide Perovskite can be used as gain materials.

Initially, the gain layer can be sandwiched between two top and bottom mirrors, Bragg reflectors, which simply form the vertical cavity surface emitting laser (VCSEL). Compared to the VCSEL, which can be obtained easily, whispering-gallery mode (WGM) microdisk lasers (MDLs) utilize successive total internal reflection along the disk circumference and provide high cavity quality factor (Q) and small mode volume (V) for integration of miniaturized devices (Mccall *et al.*, 1992).

One of the NIR solid-state nanolasers based on organic–inorganic Perovskite  $\text{CH}_3\text{NH}_3\text{PbI}_{3-x}\text{X}_x$  (X = I, Br, Cl) nanoplatelets were studied by Zhang *et al.*, 2014. They used organic–inorganic lead halide Perovskite nanoplatelets as microdisks that support WGM. By using a facile one-step solution self-assembly method, Liao *et al.* synthesized the  $\text{CH}_3\text{NH}_3\text{PbBr}_3$  MDs and WGM modes were achieved (Liao *et al.*, 2015). The distributed feedback (DFB) cavity structure was achieved by Saliba *et al.* 2016.

Nanowire structure has been applied in solar cells for a long time. (Yu *et al.*, 2016). Nanowire lasers are also believed to achieve high gain and strong confinement of photonic modes guided along the axial direction. Zhu *et al.* reported a lead halide Perovskite nanowire laser with lasing thresholds of  $220 \text{ nJ cm}^{-2}$  and high quality factor up to around 3600 (Zhu *et al.*, 2015). This work shows that solution processed lead halide Perovskite materials with its unique optical properties have great potential to be applied in lasers. Meanwhile, the stability of Perovskite also influences the devices performance and many modification methods were applied in improving the stability of Perovskite lasers. A water-resistant Perovskite polygonal microdisk laser was fabricated by Zhang *et al.* 2016. By embedding water-resistant polymer thin-film with high flexibility and transmission onto polygonal microdisks, this structure was an excellent built-in WGM micro resonator for lasing. The polymer can prevent water and moisture from Perovskite microcrystalline for improving the water resistance of the devices. Aiming to increasing the quality factor, nanostructured hybrid Perovskites have been also investigated, for example, Perovskite microcrystal laser, Perovskite microrod laser and Perovskite quantum dot LEDs have been obtained and it is a good example for the chance of applying Perovskite quantum dots in lasers. As discussed



above, the organic–inorganic hybrid Perovskite laser can be realized by different cavity configurations and it is important to improve the stability of Perovskite materials and progressing on patterned technology in order to achieve better performance of corresponding laser. The Perovskite laser devices can be applied in many fields like display, sensor, and lab-on-chip system in the future.

### 4.3 PHOTODETECTORS

Photodetectors are important optoelectronic devices for imaging, communication, automatic control, and biomedical sensing (Sun *et al.*, 2018). The organic–inorganic hybrid Perovskite materials have potential abilities to sense the spectra from visible to NIR, and even to X-ray, which is very competitive to other material systems for photodetectors. Organic–inorganic hybrid Perovskite photodetectors are mainly fabricated by solution processing methods owing to its low cost and suitability for room temperature processing (Wang *et al.*, 2016). These features are very crucial for the fabrication of flexible photodetectors. Normally, organic–inorganic hybrid Perovskite photodetectors are fabricated in a photoconductor, photodiode, or phototransistor structure (Li *et al.*, 2015).

In order to decrease defects and grain boundaries in 3D bulk crystals, researchers attempted to synthesis 2D Perovskite nanoflakes. (Dou *et al.*, 2015). While synthesis of 2D Perovskite faced many problems such as poor chemical stability, fast crystallization rate, and the intrinsically non-van der Waals-type 3D characteristics of Perovskite, Liu *et al.* prepared 2D  $\text{CH}_3\text{NH}_3\text{PbX}_3$  Perovskite as thin as a single unit cell through a combined solution process and vapor-phase conversion method (Liu *et al.*, 2016). In their study, the current can be enhanced significantly and high photo responsivities of 22 and 12  $\text{A W}^{-1}$  were obtained with a voltage bias of 1 V. The excellent optical properties make the 2D Perovskite a promising candidate for high performance photodetectors.

Hybrid Perovskite single crystals are also ideal X-ray and gamma-ray detecting materials owing to their large mobilities, carrier lifetime and high atomic numbers of Pb, I, and Br. Wei *et al.* fabricated a single crystal hybrid Perovskite X-ray photodetector. Under continuum X-ray energy up to 50 KeV, the detection efficiency was up to 16.4% at near zero bias which is four times higher than the sensitivity achieved with  $\alpha$ -Se X-ray detectors (Wei *et al.*, 2016). Recently, Wei *et al.* have developed a hybrid Perovskite X-ray photodetector.

The first visible-blind UV hybrid Perovskite photodetector was realized by Adinolfi *et al.* 2016. Based on an  $\text{MAPbCl}_3$  single crystal, the detector achieved response times of 1 ms and showed a rising edge positioned at  $\approx 420$  nm. This shows that the organic–inorganic hybrid Perovskite materials have excellent and adjustable spectra tunability.

A self-powered structure represents a new type of photodetectors that can work without power supply. They can generate electric signal on their own. The first self-powered photodetector based on organic–inorganic hybrid Perovskite was carried out by Su *et al.* 2015. After that, Yu *et al.* applied ZnO nanorod/ Perovskite heterojunction self-powered Perovskite photodetector (Yu *et al.*, 2016).

In addition, optocoupler is a common application of photodetector and plays an important role in communication, using photodetector as a part of an optocoupler was achieved by Li *et al.* 2015. In this work, a tandem OLED was used as a light source (Li *et al.*, 2015). The photodetector was fabricated by organic–inorganic hybrid Perovskite. The optocoupler exhibits rapid frequency-response in microseconds, which shows

that organic–inorganic hybrid Perovskite materials are very promising candidates for practical use in optoelectronic devices.

The organic–inorganic hybrid Perovskite photodetectors benefit from the tunable bandgap which can select the sensing spectrum of the devices. For photodetectors, it is important to control the roughness of Perovskite thin film. As previously studied, the Perovskite thin film deposited by vapor methods is better than deposited by solution methods, it is worthwhile to try vapor deposited Perovskite thin films in photodetectors (Sun *et al.*, 2018).

## 5.0 CONCLUSION AND FUTURE OUTLOOK

Advantages of PSCs which has captured tremendous attention are its; ability to fabricate large-scale transparent or semi-transparent flexible devices, simplicity of processing, easy optimization for structural design and material engineering; projected cost efficiency with superior PCE, longer electron / hole diffusion length, broad spectral absorption and high open circuit voltage, etc. With the amount of research effort underway, guided by the adherence to the issue of best practices, this technology holds great promise to addressing our energy needs in this present day energy-starved nation, Nigeria. Balancing electron and hole transporting properties of PSCs, engineering its band gap, enhancing its fill factor either by doping or by improving its morphology, replacement of Pb with Sn, use of mixed halogen Perovskites, use of composite of  $\text{TiO}_2$  and  $\text{Sb}_2\text{S}_3$ , use of  $\text{TiO}_2$  free oxides, use of CNT polymer Nanocomposites, use of layered hybrid Perovskites, employing NiO as the p-type semiconductor, processability to improve HTL and ETL layer designs and the use of several different processing techniques such as Atomic layer deposition (ALD), high pressure pressing, chemical sintering, sol-gel and electro-deposition are known alternative optimization methods that can improve the efficiency and stability of PSCs devices.

Besides these, organic-inorganic hybrid Perovskite materials have also obtained a tremendous attention in the application of alternative optoelectronic devices such as LEDs, Lasers and photodetectors. This became possible owing to organic-inorganic hybrid Perovskite materials excellent optoelectronic properties such as long carrier diffusion lengths, high charge-carrier mobility, low excitonic binding energy, and bandgap tunability.

The development of Perovskite LEDs opens new opportunities for cost-effective and efficient light emitting devices and also influenced the application of organic–inorganic Perovskite materials in lasers. Additionally, the most desired optical properties and facile preparation methods of Perovskite films also make them great alternatives for applications in photodetectors. Promising devices have been for photo detection from NIR to visible spectrum, and more recently, even for X-ray and gamma rays. As a potential candidate for future optoelectronic devices, organic–inorganic hybrid Perovskite materials must overcome the obstacles on the way to massive industry production. Researchers should also focus on improving the competitiveness of solar power against both conventional and other renewable energy sources. Hopefully, more research efforts will be dedicated toward PV technologies in the near future to enhance their efficiency, stability, manufacturability, and availability, to reduce balance-of-system (BOS) costs and reduce the costs of modules. Despite the challenges, organic inorganic metal halide Perovskites offer promising alternatives for developing high performance and low cost optoelectronic devices. We therefore anticipate the outstanding optoelectronic properties of LEDs systems to lead to low-cost and high performance photon sources for lighting, display and communication

technologies since low absorption losses have been noted to enable performance enhancement via photon recycling that allows outcoupling for modes guided in-plane. We hope organic-inorganic hybrid Perovskite lasers will be realized by different cavity configurations by improving the stability of Perovskite materials maybe by embedding water-resistant polymer thin film with high flexibility or synthesizing a low coherent random lasing threshold carrier density of Perovskite lasers with high quality factor and progressing on patterned technology in order to achieve better performance of corresponding laser. We also believe that organic-inorganic hybrid Perovskite photodetectors will benefit more from the tunable bandgap which can select the sensing spectrum of the devices by controlling the roughness of Perovskite thin film via vapour deposited Perovskite thin films synthesis or combination of solution process and vapour-phase conversion method. Given the great progresses made in such a short duration, these devices are expected to have a bright future.

## REFERENCES

- Abbas, H., Kottokkaran, R., Balaji, G., Samie, M., Zhang, L. and Dalal, V. L. (2015). High efficient sequentially vapor grown n-i-p  $\text{CH}_3\text{NH}_3\text{PbI}_3$  Perovskite solar cells with undoped P3HT as p-type heterojunction layer, *APL Materials*. **3**: 016105.
- Abrusci, A., Stranks, S. D., Docampo, P., Yip, H.L., Jen, A. K.Y and Snaith, H. J. (2013). High-performance Perovskite-polymer hybrid solar cells via electronic coupling with fullerene monolayers. *Nano Letters*. **(13)7** : 3124–3128.
- Adinolfi, V., Ouellette, O., Saidaminov, M. I., Walters, G., Abdelhady, A. L., Bakr, O. M. and Sargent, E. H. (2016). Fast and Sensitive Solution-Processed Visible-Blind Perovskite UV Photodetectors. *Advanced Materials*, 28, 7264. <https://doi.org/10.1002/adma.201601196>
- Bagnall, D., Chen, Y., Zhu, Z., Yao, T., Koyama, S., Shen, M., and Goto, T. (1997). Optically pumped lasing of ZnO at room temperature *Applied Physic Letters*, 1997, 70, 2230. <https://doi.org/10.1063/1.118824>
- Baodan, Z.; Sai B.; Vincent K., ...and Dawei D. (2018). High-efficiency Perovskite-polymer bulk heterostructure light-emitting diodes. *ResearchGate*.[https://www.researchgate.net/publication/324793185\\_high-efficiency\\_perovskite-polymer\\_bulk\\_heterostructure\\_light-emitting\\_diodes](https://www.researchgate.net/publication/324793185_high-efficiency_perovskite-polymer_bulk_heterostructure_light-emitting_diodes)
- Ball, J. M. and Petrozza, A. (2016). Defects in Perovskite-halides and their effects in solar cells. *Nature Energy* 1, 16149
- Bi, D., Moon, S. J., and Haggman, L. (2013). Using a two-step deposition technique to prepare Perovskite

- ( $\text{CH}_3\text{NH}_3\text{PbI}_3$ ) for thin film solar cells based on  $\text{ZrO}_2$  and  $\text{TiO}_2$  mesostructures. *RSC Advances*. (3)41: 18762–18766.
- Brenner, T. M., Egger, D. A., Kronik, L., Hodes, G. and Cahen, D. (2016). Hybrid organic—inorganic Perovskites: low-cost semiconductors with intriguing charge-transport properties. *Nature Revolution Materials* 1, 15007
- Burschka, J., Pellet, N., and Moon, S.J. (2013). Sequential deposition as a route to high-performance Perovskite-sensitized solar cells. *Nature*, (499)7458 : 316–319.
- Cha, H., Bae, S., Lee, M. and Jeon, H. (2016). Two-dimensional photonic crystal bandedge laser with hybrid Perovskite thin film for optical gain *Applied Physics Letters*, 108, 181104.
- Chen, R., Tran, T.T. D., Ng, K. W., Ko, W. S., Chuang, L. C., Sedgwick, F. G., and Chang-Hasnain, C. (2011). Nanolasers grown on silicon *Nature Photonics*, 5, 170.
- Chiang, Y.F., Jeng, J.Y., Lee, M.H., Peng, S.R. and Hsu, C.M. (2014). High voltage and efficient bilayer heterojunction solar cells based on an organic-inorganic hybrid Perovskite absorber with a low-cost flexible substrate. *Phys. Chem. Chem. Phys.*, 16: 6033-6040.
- Dawn, J. M. (2016). An introduction to Perovskite solar cells (PSCs). *ECE*. University of British Columbia – Vancouver. Retrieved on July 4<sup>th</sup> 2017 from <https://www.researchgate.net/publication/303541142>
- Dhanker, R., Brigeman, A. N., Larsen, A. V., Stewart, R. J., Asbury, J. B., and Giebink, N. C. (2014). Random lasing in organo-lead halide Perovskite microcrystal networks *Applied Physics Letter*, 105, 151112, <https://doi.org/10.1063/1.4898703>
- Di, D. et al. (2017). High-performance light-emitting diodes based on carbene-metal-amides. *Science* 356, 159–163
- Docampo, P., Ball, J. M., Darwich, M., Eperon, G. E. and Snaith, H. J. (2013). Efficient organometal trihalide Perovskite planar heterojunction solar cells on flexible polymer substrates. *Nature Communications*. (4)2761
- Dou, L., Wong, A. B., Yu, Y., Lai, M., Kornienko, N., Eaton, S. W., Fu, A., Bischak, C. G., Ma, J. ....Yang, P. (2015). Atomically thin two-dimensional organic-inorganic hybrid Perovskites. *Science*, 349, 1518. 349(6255). doi: 10.1126/science.aac7660
- Eperon, G.E., Burlakov, V.M., Docampo P., Goriely A. and Snaith, H.J. (2013). Morphological Control for High Performance, Solution-Processed Planar Heterojunction Perovskite Solar Cells. *Advanced Functional Materials* 24: 151–157. Available: <http://dx.doi.org/10.1002/adfm.201302090>.
- Ezike, C., Kana, G., & Aina, A. (2017). Progress and Prospect on Stability of Perovskite Photovoltaics. *Journal*

*of Modern Materials*, (4)1 :16-30. doi: <https://doi.org/10.21467/jmm.4.1.16-30>

Fang, Y., Dong, Q., Shao, Y., Yuan, Y. and Huang, J. (2015). Highly narrowband Perovskite single-crystal photodetectors enabled by surface-charge recombination. *Nat. Photonics* 9, 679–686

Green, M. A., Ho-Baillie, A. and Snaith, J. (2014). The emergence of Perovskite solar cells. *Nature Photon.* 8 : 506–514.

Hu, H., Wang, D. and Zhou, Y. (2014). Vapour-based processing of hole-conductor-free  $\text{CH}_3\text{NH}_3\text{PbI}_3$  Perovskite/C60 fullerene planar solar cells, *RSC Advances*, (4)55 : 28964– 28967.

Im, J.H., Kim, H.S. and Park, N.G. (2014). Morphology-photovoltaic property correlation in Perovskite solar cells: One-step versus two-step deposition of  $\text{CH}_3\text{NH}_3\text{PbI}_3$ , *APL Materials*, (2)081510.  
<https://doi.org/10.1063/1.4891275>

Jeng, J.Y., Chiang, Y.F., and Lee, M.H. (2013).  $\text{CH}_3\text{NH}_3\text{PbI}_3$  Perovskite/fullerene planar-heterojunction hybrid solar cells. *Advanced Materials*. (25)27 : 3727–3732.

Kesinro, O.R., Akinyemi, M.L. and Boyo, A.O. (2017). Advances in Perovskite-Based Solar Cells for the Proceedings of International Conference on Science and Sustainable Development (ICSSD) “The Role of Science in Novel Research and Advances in Technology” Center for Research, Innovation and Discovery, Covenant University, Nigeria. *Journal of Informatics and Mathematical Sciences* (9)2 : 485–491.

Kim, H.S., Lee, C.R., Im, J.H., Lee, K.B. and Park, N.G. (2012). Lead iodide Perovskite sensitized all-solid-state submicron thin film mesoscopic solar cell with efficiency exceeding 9%. *Scientific Reports*, 2 : 591

Kim, H.S., Im, S.H. and Park, N.G. (2014). Organolead halide Perovskite: new horizons in solar cell research. *Journal of Physical Chemistry C*, (118)11: 5615–5625.

Kojima, A., Teshima, K., Miyasaka, T., and Shirai, Y. (2006). Novel photoelectrochemical cell with mesoscopic electrodes sensitized by lead-halide compounds, in: 210<sup>th</sup> *ECS Meeting*, Cancun, Mexico, p. 397.

Kojima, A., Teshima, K., Shirai, Y. and Miyasaka, T. (2008). Novel photoelectrochemical cell with mesoscopic electrodes sensitized by lead-halide compounds (11). *ECS Meeting*. vol. 27, abstract MA2008-02.

Kojima, A., Teshima, K., Shirai, Y. and Miyasaka, T. (2009). Organometal halide Perovskites as visible-light sensitizers for photovoltaic cells. *Journal of American Chemistry Society*. 131 : 6050–6051.

Lee, M.M., Teuscher, J., Miyasaka, T., Murakami, T.N. and Snaith, H.J. (2012). Efficient hybrid solar cells based on meso-superstructured organometal halide Perovskites. *Science*. 338: 643-647.

Leijtens, T., Eperon, G.E., Pathak, S., Abate, A., Lee, M.M. and Snaith, H.J. (2013). Overcoming ultraviolet

- light instability of sensitized TiO<sub>2</sub> with meso-superstructured organometal trihalide Perovskite solar cells. *Nature Communications*. **4** : 2885
- Li, C., Lu, X., Ding, W., Feng, L., Gao, Y. and Guo, Z. (2008). Formability of ABX<sub>3</sub> (X = F, Cl, Br, I) halide Perovskites. *Acta Crystallographica B*, **64** : 702–707.
- Li, F., Ma, C., Wang, H., Hu, W., Yu, W., Sheikh, A. D. and Wu, T. (2015). Ambipolar solution-processed hybrid Perovskite phototransistors, *Nature Communications*, **6**, 8238. doi: 10.1038/ncomms9238.
- Li, D., Dong, G., Li, W. and Wang, L. (2015). High performance organic-inorganic Perovskite-optocoupler based on low-voltage and fast response Perovskite compound photodetector. *Scientific Reports*, **5**, 7902. DOI:10.1038/srep07902
- Liang, P. W., Liao, C. Y., Chueh, C. C., Zuo, F., Williams, S. T., Xin, X. K., Lin, J. and Jen, A. K. Y. (2014). Additive enhanced crystallization of solution-processed Perovskite for highly efficient planar-heterojunction solar cells. *Advance Materials*, **26** : 3748-3754.
- Liu, M., Johnston, M.B., Snaith, H.J. (2013). Efficient Planar heterojunction Perovskite Solar Cells by vapour deposition, *Nature*, **501**: 395–398.
- Liu, D. and Kelly, T.L. (2014). “Perovskite solar cells with a planar heterojunction structure prepared using room-temperature solution processing techniques,” *Nature Photonics*, **(8)2** : 133–138.
- Liu, J., Xue, Y., Wang, Z., Xu, Z.Q., Zheng, C., Weber, B.,..... Bao, Q. (2016). Two-Dimensional CH<sub>3</sub>NH<sub>3</sub>PbI<sub>3</sub> Perovskite: Synthesis and Optoelectronic Application. *ACS Nano*, **10(3)**:3536-42. doi: 10.1021/acsnano.5b07791
- Luther M. and Ranjit T. K. (2014). Versatility of Evaporation-Induced Self-Assembly (EISA) Method for Preparation of Mesoporous TiO<sub>2</sub> for Energy and Environmental Applications. *Materials*, **7** : 2697-2746; doi:10.3390/ma7042697. ISSN 1996-1944. Retrieved on December 2017 from: [www.mdpi.com/journal/materials](http://www.mdpi.com/journal/materials)
- Mailoa, J. P., Bailie, C. D. and Johlin, E. C. (2015). A 2-terminal Perovskite/silicon multijunction solar cell enabled by a silicon tunnel junction. *Applied Physics Letters*. **(106)12** : 121105.
- Malinkiewicz, O., Yella, A. and Lee, Y.H. (2014). Perovskite solar cells employing organic charge-transport Layers. *Nature Photonics*, **(8)2** : 128–132.
- Mccall, S., Levi, A., Slusher, R., Pearton, S. and Logan, R. (1992). Whispering-gallery mode microdisk lasers *Applied Physics Letter*, **60**, 289, <https://doi.org/10.1063/1.106688>
- Muhammad, I. A., Amir, H., and Syed, S. J. (2015). Perovskite Solar Cells: Potentials, Challenges, and Opportunities. *Hindawi Publishing Corporation International Journal of Photoenergy*,



(2015)592308-??? : 13 doi : 10.1155/2015/592308

Noh, J.H., Jeon, N.J., Choi, Y.C., Nazeeruddin, M.K., Grätzel, M. and Seok, S.I. (2013). Nanostructured  $\text{TiO}_2/\text{CH}_3\text{NH}_3\text{PbI}_3$  heterojunction solar cells employing spiro-OMeTAD/Co-complex as hole-transporting Material. *Journal of Materials Chemistry A*, (1)38 : 11842–1184.

Olopade, M. A., Oyebola, O. O., Adewoyin, A. D., Emi-Johnson, D. O. (2015). Modeling and Simulation of CZTS/CTS Tandem Solar Cell using wxAMPS Software. Department of Physics, University of Lagos, Akoka, Lagos, Nigeria. 978-1-4799-7944-8/15©IEEE.

Pang, S., Hu, H., Zhang J., Lv, S., Yu, Y., Wei, F., Qin, T. and Cui, G. (2014).  $\text{NH}_2\text{CH}=\text{NH}_2\text{PbI}_3$ : an alternative organolead iodide Perovskite sensitizer for mesoscopic solar cells. *Chemistry of Materials*, (26)3 : 1485–1491. **Doi** : 10.1021/cm404006p

Paola, V., Jagadish, K. S., and Arri, P. (2017). Hole-Transporting Materials for Printable Perovskite Solar Cells. *Materials*, **10** : 1087-????; doi:10.3390/ma10091087

Rong, L., Liu, L., Mei, A., Li, X., and Han, H. (2015). Beyond efficiency: the challenge of stability in mesoscopic Perovskite solar cells. *Advance Energy Materials*. **5** : 1501066.

Service, R.F. (2014). Energy technology: Perovskite solar cells keep on surging. *Science*, (344)6183 : 458.

Snaith, H.J. (2013). Perovskites: the emergence of a new era for low-cost, high-efficiency solar cells. *Journal of Physical Chemistry Letters*, **4** : 3623 – 3630.

Song, T., Chen, Q., Zhou, H., Jiang, C., Wang, H., Yang, Y., Liu, Y., You, J., and Yang, Y. (2015). Perovskite solar cells: film formation and properties. *Journal of Materials Chemistry A*, Retrieved on January 5<sup>th</sup> 2017 from <http://www.rsc.org/materialsA>

Stoumpos, C.C., Malliakas, C.D. and Kanatzidis, M.G. (2013). Semiconducting tin and lead iodide Perovskites with organic cations: phase transitions, high mobilities, and near-infrared photoluminescent properties. *Inorganic Chemistry*, (52)15 : 9019–9038.

Su, L., Zhao, Z. X., Li, H. Y., Yuan, J., Wang, Z. L., Cao, G. Z., and Zhu, G. (2015). High-Performance Organolead Halide Perovskite-Based Self-Powered Triboelectric Photodetector, *ACS Nano*, 2015, 9 (11), pp 11310–11316, DOI: 10.1021/acsnano.5b04995

Sun, J., Wu, J., Tong, X., Lin, F., Wang, Y., and Wang, Z.M. (2018). Organic/Inorganic Metal Halide Perovskite Optoelectronic Devices beyond Solar Cells. *Advanced Science*,(5) 1700780, DOI: 10.1002/advs.201700780

Wang, J. et al. (2015). Interfacial control toward efficient and low-voltage Perovskite light-emitting diodes. *Advance Materials* 27, 2311–2316

Wang, D., Wright, M., Elumalai, K.N., and Uddin, A. (2016). Stability of Perovskite solar cells. *Solar Energy Materials and Solar Cells*. **147** : 255-275. <http://dx.doi.org/10.1016/j.solmat.2015.12.025>

Wang, Y., Xia, Z., Du, S., Yuan, F., Li, Z., Li, Z., Dai, Q., Wang, H., Luo, S., Zhang, S., and Zhou, H. (2016). Solution-processed photodetectors based on organic-inorganic hybrid Perovskite and nanocrystalline graphite *Nanotechnology*, 27, 175201, <https://doi.org/10.1088/0957-4484/27/17/175201>

Wei, H., Fang, Y., Mulligan, P., Chuirazzi, W., Fang, H-H., Wang, C., ... Huang, J. (2016). Sensitive X-ray detectors made of methylammonium lead tribromide Perovskite single crystals. *Nature Photonics*, 10(5), 333-+. DOI: 10.1038/NPHOTON.2016.41

Weller, M. T., Weber, O. J., Frost, J. M. and Walsh, A. (2015). Cubic Perovskite structure of black formamidinium lead iodide,  $\alpha$ -[HC(NH<sub>2</sub>)<sub>2</sub>]PbI<sub>3</sub>, at 298 K. *Journal of Physical Chemistry Letter* 6, 3209–3212

Xiao, Z., Bi, C. and Shao, Y. (2014). Efficient, high yield Perovskite photovoltaic devices grown by inter diffusion of solution-processed precursors tacking layers. *Energy & Environmental Science*, (7)8 : 2619–2623.

Xiao, Z. et al. (2017). Efficient Perovskite light-emitting diodes featuring nanometre-sized crystallites. *Nature Photonics* 11, 108–115

Xing, G., Mathews, N., Lim, S. S., Yantara, N., Liu, X., Sabba, D., Gratzel, M., Mhaisalkar, S. and Sum, T. C. (2014). Low-temperature solution-processed wavelength-tunable Perovskites for lasing. *Nature Materials*, 13(5):476-80. doi: 10.1038/nmat3911.

Yablonovitch, E. (2016). Lead halides join the top optoelectronic league. *Science* 351, 1401

Yang, X. et al. (2018). Efficient green light-emitting diodes based on quasi-two-dimensional composition and phase engineered Perovskite with surface passivation. *Nature Communications*, 9, 570

You, J., Hong, Z., Yang, Y., Chen, Q., Cai, M. and Yang, Y. (2014). Low-temperature solution-processed Perovskite solar cells with high efficiency and flexibility. *ACS Nano*, **8** : 1674-1680.

Yu, Z. and Sun, L. (2015). Recent progress on hole-transporting materials for emerging organometal halide Perovskite solar cells. *Advance Energy Materials*. **5**: 1500213.

Yu, P., Wu, J., Liu, S., Xiong, J., Jagadish, C., and Wang, Z. M. (2016). Design and fabrication of silicon nanowires towards efficient solar cells. *Nano Today*, 11, 704.

Yu, J., Chen, X., Wang, Y., Zhou, H., Xue, M., Xu, Y., ... Wang, H. (2016). A high-performance self-powered broadband photodetector based on a CH<sub>3</sub>NH<sub>3</sub>PbI<sub>3</sub> Perovskite/ZnO nanorod array heterostructure. *JOURNAL OF MATERIALS CHEMISTRY C*, 4(30), 7302-7308. DOI: 10.1039/c6tc02097f

Yuan, M. et al. (2016). Perovskite energy funnels for efficient light-emitting diodes. *Nature Nanotechnology*, 11, 872–877

Zhang, W. *et al.* (2015). Ultrasoft organic–inorganic Perovskite thinfilm formation and crystallization for efficient planar heterojunction solar cells. *Nature Communication*, 6 : 6142.

Zhang, H., Liao, Q., Wang, X., Yao, J., and Fu, H. (2016). Water-Resistant Perovskite Polygonal Microdisks Laser in Flexible Photonics Devices *Advanced Optical Materials*, 4, 1718,  
<https://doi.org/10.1002/adom.201600335>

Zhou, H., Chen, Q. and Li, G. (2014). Interface engineering of highly efficient Perovskite solar cells. *Science*, (345)6196 : 542–546

IJSER